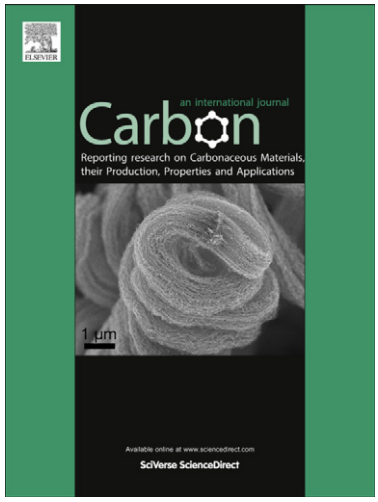

Dielectric Properties of Carbon Nanofibre/Alumina Composites

Lucia Fernandez-Garcia, Marta Suárez, Jose Luis Menéndez, Carlos Pecharromán, Dmitry Nuzhnyy, Viktor Bovtun, Maxim Savinov, Martin Kempa, Jan Petzelt

PII: S0008-6223(13)00119-X
DOI: http://dx.doi.org/10.1016/j.carbon.2013.01.086
Reference: CARBON 7824

To appear in: *Carbon*

Received Date: 13 August 2012
Accepted Date: 30 January 2013

Please cite this article as: Fernandez-Garcia, L., Suárez, M., Menéndez, J.L., Pecharromán, C., Nuzhnyy, D., Bovtun, V., Savinov, M., Kempa, M., Petzelt, J., Dielectric Properties of Carbon Nanofibre/Alumina Composites, *Carbon* (2013), doi: http://dx.doi.org/10.1016/j.carbon.2013.01.086

DIELECTRIC PROPERTIES OF CARBON NANOFIBRE/ALUMINA COMPOSITES

Lucia Fernandez-Garcia[a], Marta Suárez[a], Jose Luis Menéndez[a1], Carlos Pecharromán[b], Dmitry Nuzhnyy[c], Viktor Bovtun[c], Maxim Savinov[c], Martin Kempa[c], Jan Petzelt[c]

[a]*Centro de Investigación en Nanomateriales y Nanotecnología (CINN). Consejo superior de Investigaciones Científicas (CSIC) – Universidad de Oviedo (UO) – Principado de Asturias. Parque Tecnológico de Asturias, 33428 Llanera, (Asturias), Spain.*

[b]*Instituto de Ciencia de Materias de Madrid, Calle Sor Juana Inés de la Cruz 3, 28049 Cantoblanco, Madrid, Spain.*

[c]*Institute of Physics, Academy of Sciences of the Czech Republic,*

Na Slovance 2, 18221 Praha 8, Czech Republic.

ABSTRACT

Carbon nanofibre (CNF)/Al_2O_3 composites with concentrations between 1 and 9 vol.% of CNF were prepared by the traditional ceramic

[1]*Corresponding author. Tel/Fax: +34 985733644. E-mail address: jl.menendez@cinn.es (J.L. Menendez)

processing route followed by spark plasma sintering. The dielectric properties of these composites have been studied in a broad frequency range from mHz to the infrared range. Unlike conventional composites, the percolation threshold in this system is more complex depending on the particles topology. Positive and negative variations by several orders of magnitude in the low frequency ac conductivity have been detected for concentrations near the threshold at ~2 vol.% of CNF. To explain these results, a modified percolation model has been proposed which takes into consideration the effect of the concentration of the filler on the microstructure of the composite.

1. INTRODUCTION

Composites formed by a dielectric ceramic matrix and a conductive filler are very interesting materials since their physical properties, such as optical, electrical and magnetic properties as well as tribological, corrosion-resistance and wear properties can be tailored, which makes them attractive for many new electronic, optical, magnetic and structural applications [1-4]. In particular, the introduction of carbon based nanoparticles, such as CNTs or CNFs, in polymeric or ceramic matrices has led to the development of materials for a wide variety of new applications [5,6], and devices based on tunable electrical conductivity [7], piezoresistivity [8], magnetoresistivity [9] or electromagnetic shielding [10,11]. However, from

a technological point of view, CNFs offer several advantages compared to CNTs. CNTs are subject to much stronger Van der Waals forces than CNFs, so it becomes necessary to disperse or functionalize CNTs, increasing production costs. Also, the cost of the CNFs is in the range of some hundred euros per kg, whereas the cost of CNTs rises to hundreds of euros per gram. Besides their functional aspects, machining of ceramic materials is quite a hard and expensive task. In this regard, the use of Electro Discharge Machining (EDM) allows cutting very complicated pieces. However, EDM requires bulk ceramic items with an acceptable level of conductivity [12]. In this regard, the inclusion of CNFs is a convenient solution. Due to the shape of these nanoparticles, just a few per cent of these fibers are required to turn dielectric ceramics into conducting composites, but keeping unchanged most of the mechanical properties of the ceramic materials.

In order to prepare efficient composites, it is necessary to control both mechanical and electric properties by keeping the carbon phase concentration as low as possible. In this regard, it is well known that the minimum amount of the conductive phase required to turn the whole composite conducting is determined by the percolation threshold. This mathematical concept states that inclusions inside a matrix remain isolated just until the critical concentration is reached. At this point all particles

become connected, forming the so-called infinite cluster. Conductivity and dielectric constant show a critical behavior when the fraction of the conducting phase reaches the percolation threshold [13,14], which has been the subject of interest of many studies [15-17]. Specifically, electric conductivity shows a steep change by several orders of magnitude near this percolation threshold from the value corresponding to the dielectric component to that of the conducting phase. According to the percolation theory, as the concentration of the conductive phase in a dielectric matrix rises, the composite keeps its insulating character but its resistivity slightly decreases. However, once the critical concentration is reached, the material becomes dc conducting. It has been shown both experimentally and theoretically that the percolation threshold strongly depends on the aspect (length-to-diameter) ratio of the conductive particles [18-20]. Hence, it is not surprising that a number of experimental studies have verified the potential of CNTs as a conductor filler resulting in very low percolation thresholds [21,22] and most of the studies have been carried out with CNTs in polymer matrices [23-26].

According to the classical percolation model, it is implicitly assumed that topology of the composite is not modified when the concentration of one of the components varies. However in real ceramic systems, fillers may strongly modify the growth rate. In fact, it is well known that the presence

of inclusions modifies the surface energy of the ceramic grains. When the particle size of the filler is much smaller than that of the matrix grains, the small particles are able to hinder the grain growth of the larger ones, inducing the so-called pinning effect [27]. A similar effect has been previously observed in carbon/polymeric composites [28].

In this work the electrical properties of spark plasma sintered CNF-alumina composites are studied in a broad spectral range, from mHz to the infrared range, for concentrations of CNFs between 1 and 9 vol.%. The conduction percolation threshold and the changes in the microstructure of the composites are discussed. Besides the technological importance of these systems, alumina/CNF can be considered to be a model to study the correlation between conductive and microstructural properties of ceramic carbon nanocomposites.

2. EXPERIMENTAL

CNF-alumina powders having concentrations between 1 and 9 vol.% of CNF were prepared as follows: the raw materials, Al_2O_3 (Taimei TM-DAR, >99.99% purity) with an average particle size of around 150 nm and CNFs (Grupo Antolín Ingeniería) with the fiber diameter around 50 nm and fibre length up to 30 μm, were mixed in propanol and ball milled for 1 hour. The mixed powders were uniaxially pressed at 30 MPa and sintered at a heating rate of $50^{o}C \cdot min^{-1}$ in a spark plasma sintering apparatus (FCT-HP D25/1) under an applied pressure of 80 MPa and in vacuum (10^{-1} mbar). The final sintering temperature was 1500 ºC and the holding time 1 min.

Powder X-ray diffraction analysis (D8 Advance, BRUKER) was used to determine the crystalline phases of the sintered samples. The microstructure of the sintered samples was characterized by Field Emission Scanning Electron Microscopy (FESEM) on a QUANTA FEG 650. Dielectric properties of the samples were studied by the infrared (IR) reflectivity (Fourier transform IR spectrometer Bruker IFS 113v, specular reflection attachment), time-domain THz transmission spectroscopy (laboratory-made spectrometer based on an amplified Ti-sapphire femtosecond laser system [29]), microwave (MW) dielectric measurements

(open-end coaxial technique with Agilent E8364B vector network analyzer in the 200 MHz – 8 GHz range) and standard low-frequency dielectric measurements (High Performance Frequency Analyzer Novocontrol Alpha-AN in the 10^{-2} – 10^{7} Hz range).

3. RESULTS AND DISCUSSION

X-ray diffraction analysis shows that, even at the highest CNF concentration (Fig.1), only the diffraction peaks corresponding to alumina and CNFs are present, indicating that no reaction has taken place.

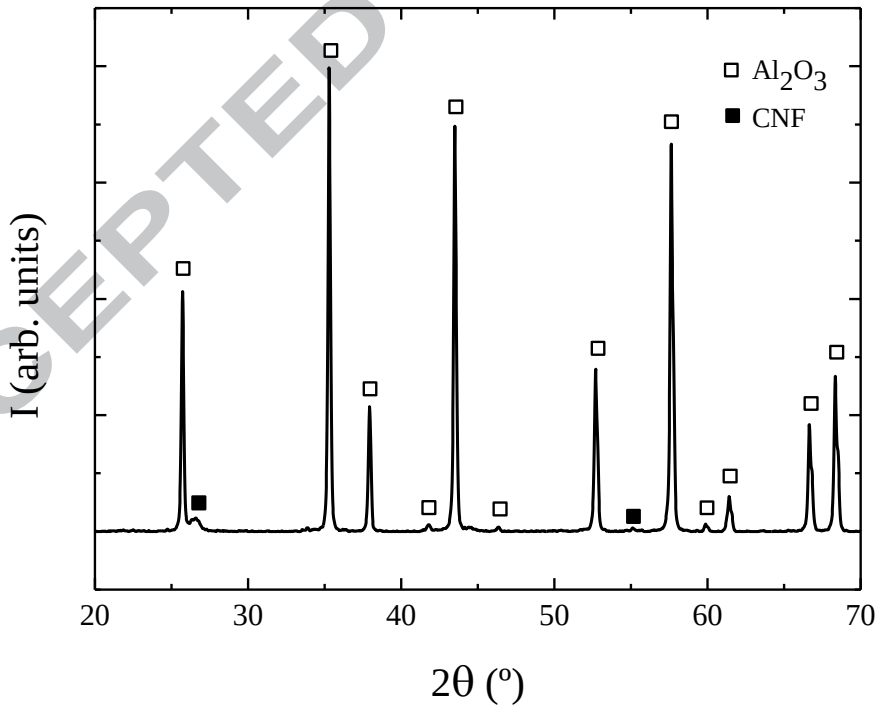

Figure 1. X-ray diffractograph for the sample with the highest (9 vol.%) CNF content.

Field Emission Scanning Electron Microscopy images (Fig. 2a-c) show large differences in the Al_2O_3 grain sizes and CNF distribution as a function of the CNF concentration in the samples. The sample with 1 vol.% CNF has an average alumina grain size around 6 μm (Fig. 2a) while once the CNF content increases to 2 vol.%, the alumina grain size abruptly decreases below 2 μm (Fig. 2b). For larger CNF contents, the grain size shows a smooth decrease (Figs. 2a-d). This indicates that the CNFs act as pinning centers hindering the Al_2O_3 grain growth. On the other hand, in figures 2a to 2d it can be seen that fibers are placed in the Al_2O_3 grain boundaries and preferentially located in triple points. The decrease in the alumina grain size when the CNF content increases from 1 to 2% leads to a larger availability of positions for the CNFs to be located in the grain boundaries. In other words, the CNF content increases globally in the whole composite, whereas locally (in the grain boundaries) the CNF concentration decreases. As a consequence, the electromagnetic properties of the composites will become modified as shown below.

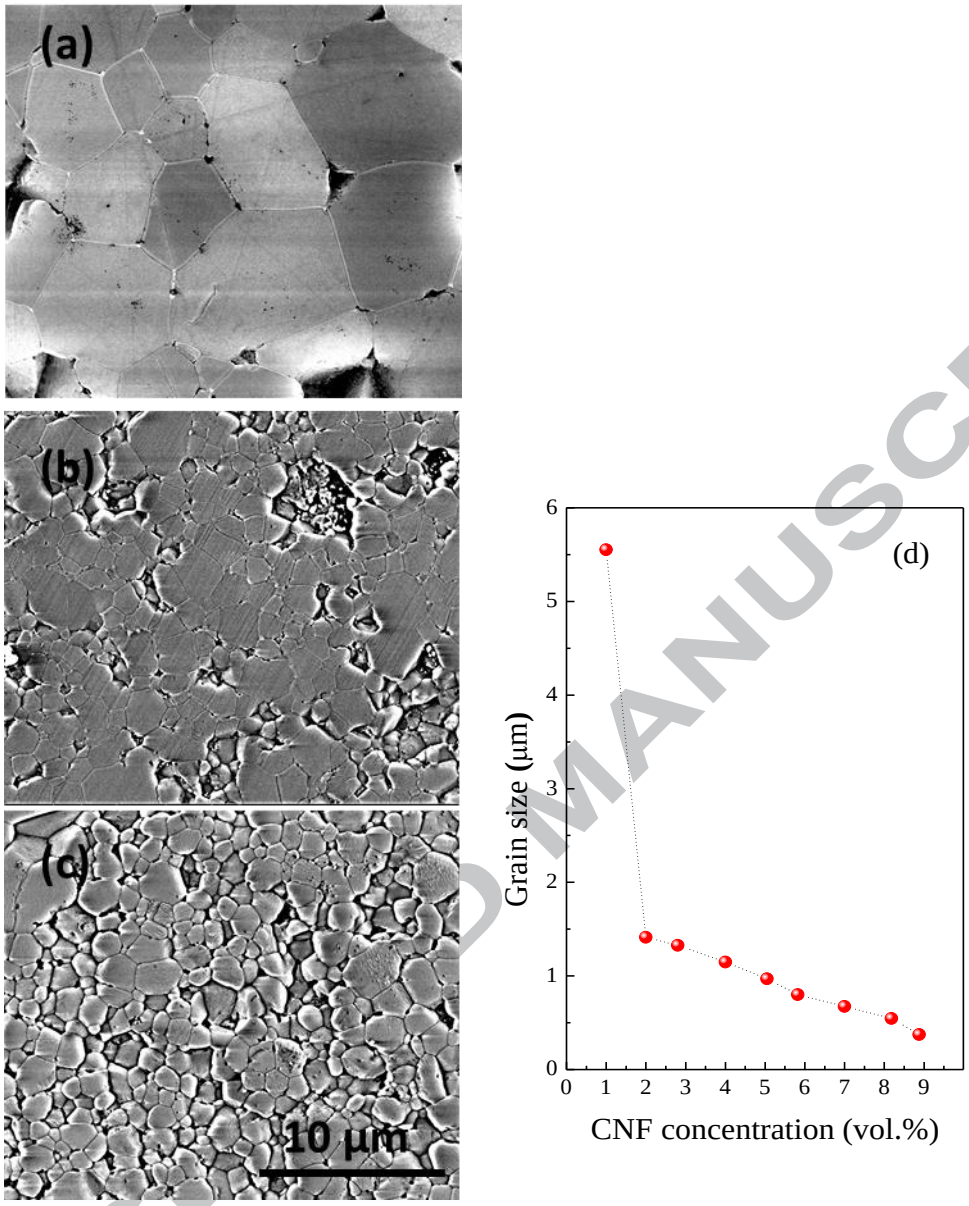

Figure 2. FESEM images of (a) 1 vol.%, (b) 2 vol.%, (c) 3vol.% of CNF composites and (d) alumina grain size vs. CNF volume concentration.

The near normal room-temperature IR specular reflectance spectra of polished surfaces of CNF-Al_2O_3 samples in the 30-3000 cm^{-1} range are plotted in Fig. 3. As alumina is strongly birefringent in this region, the effective dielectric constant of the nanocomposites has three contributions:

two given by the alumina (ordinary and extraordinary components of the dielectric tensor) plus that of the CNFs. In the case of the oxidic phase, the low-frequency IR spectral region is dominated by strong resonances due to optical phonons present. Moreover, as alumina is a uniaxial optical material (R3c space group), group theory predicts that the response along the ordinary axis presents 4 E_u and 2 A_{2u} modes for the extraordinary axis [30]. Therefore, the IR spectra of near-dense alumina composites (as well as in hematites [31] or anatase [32]) are mostly dominated by the relative grain orientation [33] rather than the CNF content. In figure 3 it is seen that, although all samples have similar spectra dominated by two strong bands in the 400–500 and 500-900 cm^{-1} (corresponding to the 4 E_u and 2 A_{2u} modes) range, not all of them exhibit the same behavior.

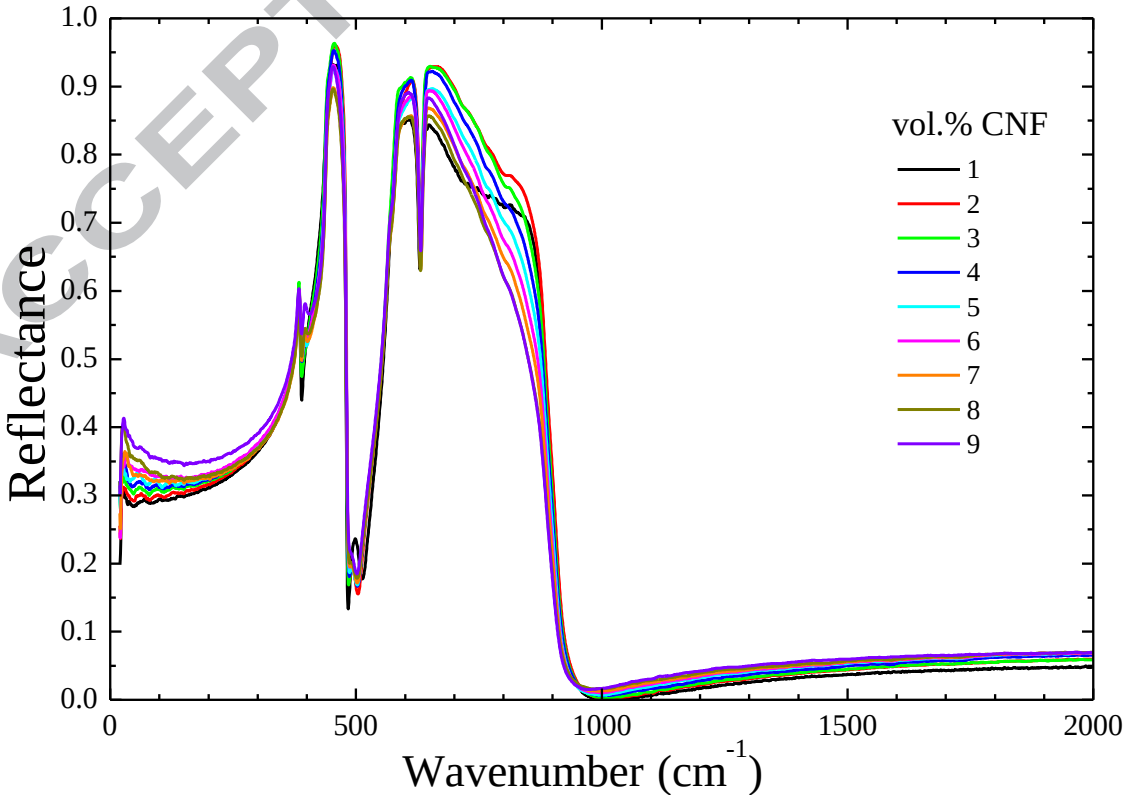

Figure 3. Reflectivity spectra in the IR range of Al_2O_3-CNF composites.

In particular, zooming in the 480-540cm^{-1} region (Fig. 4) shows a different behavior of the 1 vol.% CNF sample compared to the other samples. At a first glance one can suppose that the carbon content is responsible of this change. However, it should be noted that the effective refractive index of carbon materials, as, by instance graphite [34,35], is smaller than this of alumina precisely in the IR reststrahlung region. Therefore the only relevant role of CNF in this spectral region is the modification of the alumina grains. In this sense, the study of the IR reflectivity of pure alumina ceramics and its modeling using different effective medium models has revealed that the feature around 500 cm^{-1} is related to the grain size and topology of the ceramics [31]. It should be noted that a similar peak also appears in α-Fe_2O_3 (which is isostructural with the α-Al_2O_3) where it was attributed to the geometrical interaction between the adjacent longitudinal E_u and A_{2u} modes. The position and shape of this peak are very sensitive to the particle shape. In the case of 1 vol.% CNF sample, the reflectance maximum is compatible with a spherical grain shape. However, for higher CNF concentrations, in which the pinning effect modifies the alumina growth rate, matrix grains change their spherical shape to, very likely, a tabular shape. This is related to a different structure of this sample, which correlates well with the FESEM

images, in which much larger grain sizes were found for the sample of 1vol.% CNF. It should be reminded that alumina grains present an isometric aspect (sphere-like geometry) for large particle size while they transform into tabular plates on decreasing their size (with the shortest axis parallel to the *c* crystallographic axis) [36-38]

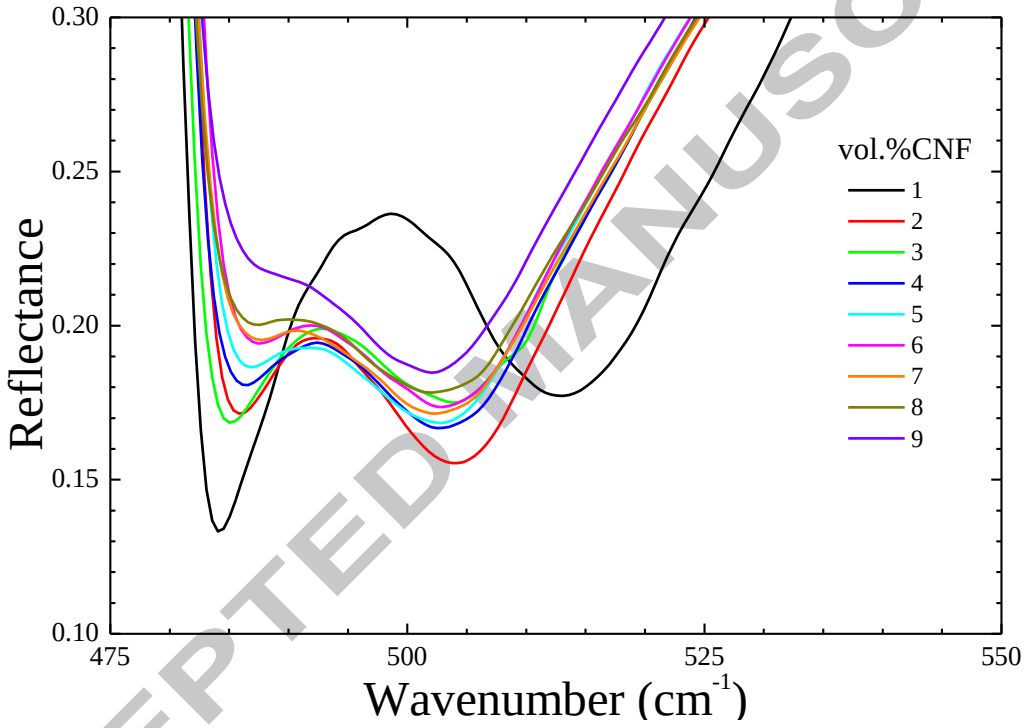

Figure 4. Reflectivity spectra in the 480-540 cm^{-1} range of the Al_2O_3-CNF samples.

The room temperature conductivity spectra in a broad frequency range of 10^{-2}–$2.6 \cdot 10^{12}$ Hz are presented in Fig. 5. The dielectric response of Al_2O_3-CNF compounds was measured at low, MW and THz frequencies. The standard low-frequency capacitance measurements were carried out with Ag electrodes deposited on both sides of the samples and the complex

dielectric response in the range of 10^{-2}–10^{6} Hz was obtained. Open-end coaxial technique was used in the 200 MHz – 8 GHz range. After that, all the samples were thinned down to ~0.5 mm and the time-domain THz transmission spectroscopy [39] was used to measure the complex transmission from which the complex dielectric response was directly calculated in the range of 0.15 – 2.6 THz.

The ac conductivity spectra are shown in Fig. 5a. All the samples show a conductivity plateau at low frequencies, which in the samples with percolated conductivity should correspond to the dc conductivity. The plateau should broaden with increasing CNF concentration, but our data are somewhat cut on approaching 1 MHz since on increasing conductivity the instrumental resonance due to leads inductance is approaching. Moreover, for higher conductivity near 10^{-2} S/cm the sample resistance becomes comparable with the contact leads resistance so that the conductivity saturates for the CNF content higher than ~5 vol.%. At higher frequencies the conductivity starts further increasing and tends to some saturation in the IR range (above the THz range). In Fig. 5b we present the corresponding real permittivity data, measured in the same frequency range.

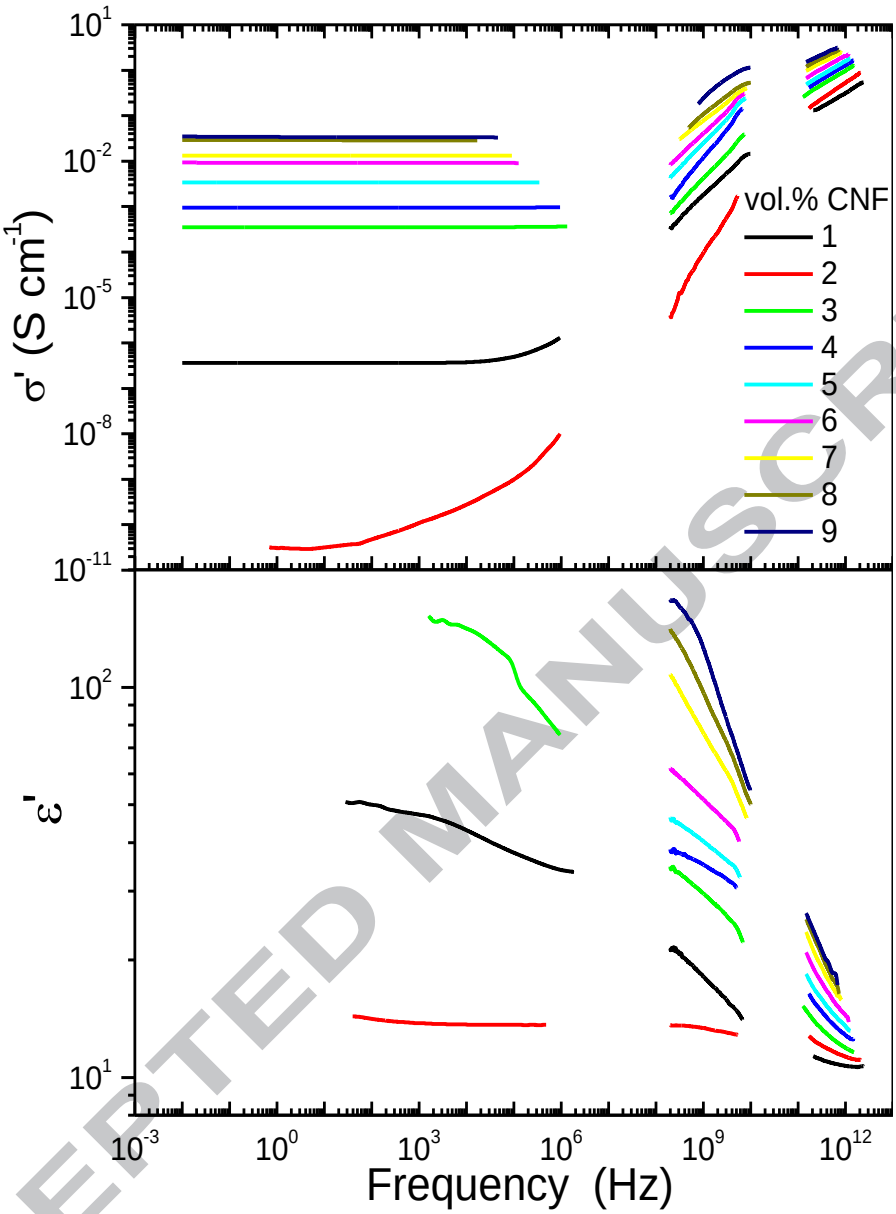

Figure 5. (a) ac conductivity of Al_2O_3-CNF samples and (b) real part of the complex permittivity of Al_2O_3-CNF samples.

As shown, the permittivity increases with decreasing frequency and increasing CNF concentration. At low frequencies the measurements are reliable only at low concentrations (up to 3 vol.% CNF), since in order to obtain reliable permittivity data the losses should not become too high (tanδ should not increase above ~100). Let us note that the increase in

permittivity even above the percolation threshold is a usually observed feature connected with the increasing conductivity vs. frequency behavior via Kramers-Kronig relations [40]. It indicates that the effective bulk conductivity of the neat CNF is not of a Drude-metal type, but rather of a universal disordered conductor type [41] due to averaging of the strongly anisotropic conductivity of the graphitic carbon [42,43].

The most remarkable feature shown in figure 5a is that the 2 vol.% CNF sample shows a smaller conductivity than the 1 vol.% CNF sample. This feature is not due to any sample labeling errors or a faulty processing, but it actually corresponds to a physical phenomenon which can be found in ceramic-based composites close to the percolation [44, 45]. Besides that, the most pronounced gap on the CNF concentration (in the log scale) appears for the dc plateaus between 2 and 3 vol. % CNF samples. In order to analyze the properties of ceramic composites with carbon inclusions around the percolation threshold, the standard percolation theory must be modified by taking into account the specific properties of this kind of composites. It should be considered that a relatively small proportion of inclusions modifies the grain growth rate of the ceramic matrix. This phenomenon, known as pinning, implies that the grain size of the matrix is reduced as the concentration of inclusions increases. In dense ceramics, in which the matrix particle size is much larger than that of inclusions, the

only available volume for the inclusions is the one around the intergranular surface (Fig. 6).

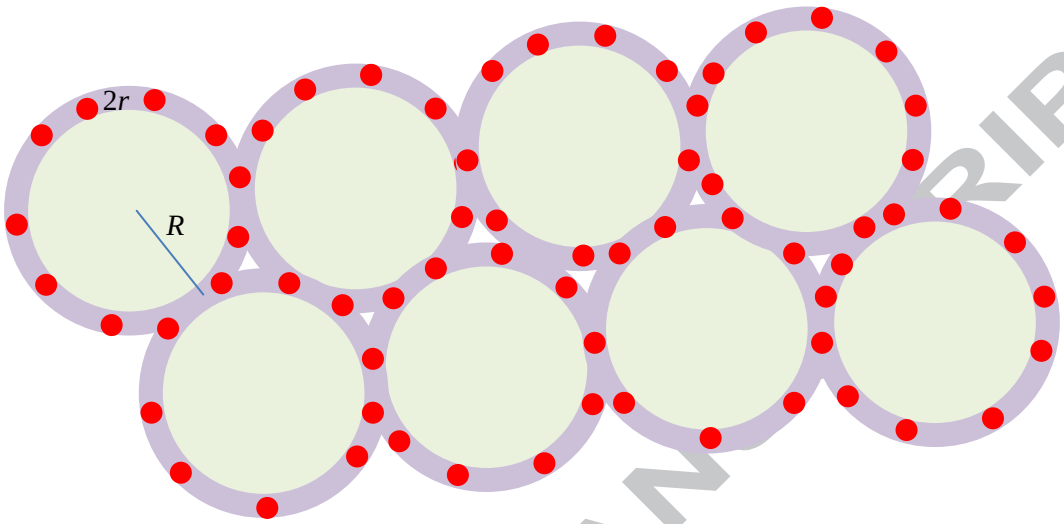

Figure 6. Schematic representation of the microstructure of a composite showing matrix grains (large clear circles), inclusions (red circles) and the space available for them (grey areas).

In this sense, it can be shown that the apparent volume concentration of the particles f_{eff} increases as a ratio of core and shell diameter (Fig. 6) [46]:

$$f_{eff} = f\,\frac{R}{3r} \tag{1}$$

Therefore, the local dielectric constant (or conductivity) of the grain boundary can be calculated using a modified effective medium model. For the model, the Bruggeman approximation was chosen [47], assuming that

the depolarization factors of both matrix and inclusions are identical so that:

$$\left(1-f_{eff}\right)\frac{\left\langle\varepsilon\right\rangle_{GB}-\varepsilon_m}{\left(1-f_c\right)\left\langle\varepsilon\right\rangle_{GB}+f_c\varepsilon_m}+f_{eff}\frac{\left\langle\varepsilon\right\rangle_{GB}-\varepsilon_p}{\left(1-f_c\right)\left\langle\varepsilon\right\rangle_{GB}+f_c\varepsilon_p}=0 \tag{2}$$

Finally, the dielectric constant of the whole composite can be calculated by the Maxwell-Garnett approach [48,49].

$$\left\langle\varepsilon\right\rangle=\left\langle\varepsilon\right\rangle_{GB}\frac{\left(1-f_m\right)+3f_m\dfrac{\varepsilon_m}{2\left\langle\varepsilon\right\rangle_{GB}+\varepsilon_m}}{\left(1-f_m\right)+3f_m\dfrac{\left\langle\varepsilon\right\rangle_{GB}}{2\left\langle\varepsilon\right\rangle_{GB}+\varepsilon_m}} \tag{3}$$

This is so because we have assumed that the matrix particles, of radius (R-$2r$) are completely coated by a layer of dielectric constant [50] $<\varepsilon>_{GB}$. This geometry determines that the relative concentration of the pure matrix phase in the composite is

$$f_m=\frac{V_m}{V}=\frac{\left[R(f)-r\right]^3}{R(f)^3}\approx 1-3\frac{r}{R(f)} \tag{4}$$

Consequently, apart from the geometric conditions it is necessary to have a good knowledge of the dielectric constant of the components. For this case we have a good insulator as it is the alumina ceramic and a conductive phase. In the case of alumina, we have assumed the simplest model for low frequency regime (for frequencies below the optical phonons)

$$\hat{\varepsilon}(\omega) = \varepsilon_r + i\frac{\sigma}{\in_0 \omega} \tag{5}$$

Where ε_r=10 and σ=10^{-11} S·cm^{-1} are the low frequency permittivity and conductivity respectively, ϵ_0=$8.85\cdot10^{-14}$ F·cm^{-1} is the vacuum permittivity and ω the angular frequency. In the case of CNF we have not found any realistic model for this material. The conductivity of this material is quite high and decreases with the frequency. In the case of an electron free plasma, the conductivity should present a ω^{-1} dependence, but in the case of carbon conductors the exponent usually presents a non-integer value. The most striking dielectric features of some carbon materials is that, at lower frequencies, both real and imaginary part of dielectric constant take positive and very high values. In fact, several works report different measurements on polymer/CNT or CNF composites [51-54] which present this increase of the real part of the permittivity at lower frequencies. Those data, which present a similar behavior to that of figure 5b referring to $\varepsilon'(\omega)$ fits quite reasonably to a power-law vs. the frequency.

$$\varepsilon'_{CNF}(\omega) \propto \omega^{-\alpha} \tag{6}$$

This type of dispersion is usually associated to a Williams-Watts model [55] and has been found in many different materials. In this sense, we have chosen a double power law complex dielectric constant as follows

$$\hat{\varepsilon}_{CNF}(\omega) \propto a\omega^{-\alpha} + i\,b\omega^{-\beta} \tag{7}$$

Where the numeric values of the coefficients are α=0.65, a= $1.6 \cdot 10^{11}$, β=1.2 and b= $5.3 \cdot 10^{17}$.

According to the micrographs of figure 2 (a, b and c) the average particle size of carbon agglomerates has been taken to be $2r$=250 nm while the alumina particle size $2R(f)$ is given in the figure 2d. The results of the calculations are shown in the figure 7 a and b. It can be seen that the theoretical conductivity of 1 and 2 vol.% CNF samples at low frequency are around 10^{-7} and 10^{-10} $S \cdot cm^{-1}$ respectively, in fair agreement with the experimental data. The rest of the samples present high values of conductivity all along the whole spectral range.

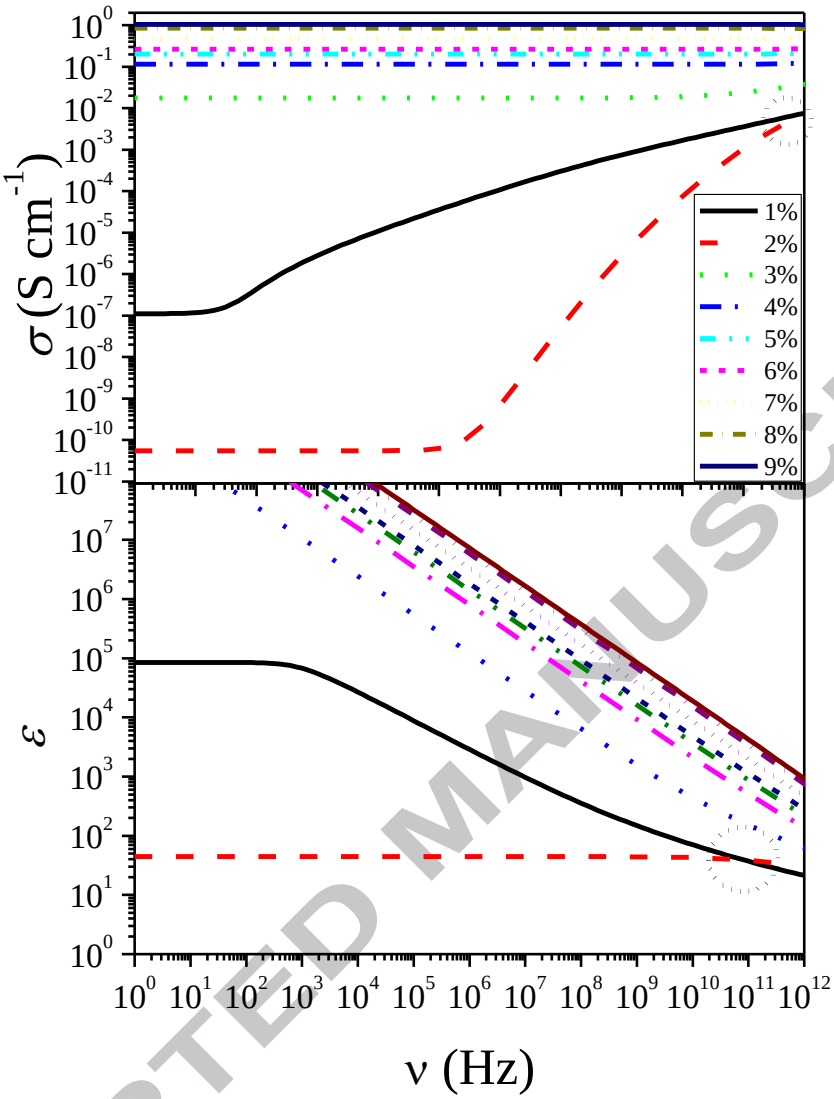

Figure 7. Simulations considering the different experimental alumina grain sizes and concentrations of CNFs.

As it happens in the experimental data, the 2 vol% CNF sample presents a much lower conductivity than the rest of the samples. A similar feature can be observed in the case of the real part of the dielectric constant, where its value is much smaller than the rest of the sample series. This can be

understood if we assume that alumina grains limit the available volume for CNF. According to equation (1), it can be inferred that 2 vol.% CNF sample presents an effective volume concentration of just f_{eff}=0.0188 where we have assumed that alumina grains grow without any hindering mechanism. According to the fitting for measurements of figures 5 a percolation threshold of $f_{c,eff}$=0.0233 were obtained, so that 2 vol.% sample is below the effective threshold concentration. However, in the case of 1vol.% CNF sample, the effective filling factor, according to equation (1), is nearly identical to effective percolation threshold. This is due to the fact that, once the CNF concentration increases above 1 vol.%, ceramic grains dimensions notably reduced due to a pinning effect caused by CNFs and this effect results in an increase of the available volume for the CNFs, so that despite the increase in the nominal concentration, CNFs fall below the percolation threshold in this specific sample. Finally in the case of the 3 vol.% CNF and above, conductivity and permittivity take again values compatible with a percolated network of carbon particles.

4. CONCLUSIONS

The study of the dielectric properties of Al_2O_3-CNF composites in a wide frequency range showed a dc conductivity plateau at low frequencies in all the 1-9 vol.% CNF samples with the percolation threshold near 2

vol.% of CNF. It was found that the dielectric and conductivity properties at low frequencies depend not only on the CNF concentration, but also on the grain size and topology of the composites. In particular, the pinning effect of small carbon particles on alumina grains modifies the spatial distribution of the conducting phase. This effect has a significant influence on the electromagnetic properties of this kind of composites in such a manner that actually the percolation threshold is reached twice (below 1 and close to 2 vol.% of CNF) as the result of the change of local CNF concentration.

ACKNOWLEDGMENTS

The authors acknowledge funding through projects No 2010CZ0004, MAT2009-14534, MAT2011-29174-C02-01, the Czech Science Foundation project P204/12/0232 and Czech Ministry of Education (project MP0902). L. Fernandez-Garcia acknowledges JAE Predoctoral program for PhD grant.

REFERENCES

[1] Moya JS, Lopez-Esteban S, Pecharroman C. The challenge of ceramic/metal microcomposites and nanocomposites. Progress in Materials Science 2007; 52:1017–90.

[2] Fahrenholtz WG, Ellerby DT, Loehman RE. Al2O3–Ni Composites with High Strength and Fracture Toughness. J Am Ceram Soc 2000; 83:1279–80.

[3] Tuan WH, Wu HH, Yang TJ. The preparation of AI2O3/Ni composites by a powder coating technique. J Mater Sci 1995; 30:855–9.

[4] Wang X, Padture NP, Tanaka H, Contact-damage-resistant ceramic/single-wall carbon nanotubes and ceramic/graphite composites. Nature Materials. 2004 3 539 - 544

[5] Coleman JN, Khan U, Blau WJ, Gunko YK. Small but strong: A review of the mechanical properties of carbon nanotube–polymer composites. Carbon 2006; 44: 1624-52.

[6] Kim IT, Tannenbaum A, Tannenbaum R. Anisotropic conductivity of magnetic carbon nanotubes embedded in epoxy matrices. Carbon 2011; 49:54-61.

[7] Liu Y, Gao L. A study of the electrical properties of carbon nanotube-NiFe2O4 composites: Effect of the surface treatment of the carbon nanotubes. Carbon 2005; 43:47-52.

[8] Oliva-Aviles AI, Aviles F, Sosa V. Electrical and piezoresistive properties of multi-walled carbon nanotube/polymer composite films aligned by an electric field. Carbon 2011; 49:2989-2997.

[9] Chauvet O, Benoit JM, Corraze B. Electrical, magneto-transport and localization of charge carriers in nanocomposites based on carbon nanotubes. Carbon 2004; 42:949-952.

[10] Mahmoodi M, Arjmand M, Sundararaj U, Park S, The electrical conductivity and electromagnetic interference shielding of injection molded multi-walled carbon nanotube/polystyrene composites. Carbon 2012; 50(4):1455-1464

[11] Fugetsua B, Sanob E, Sunada M, Sambongi Y, Shibuya T, Wang X, Hiraki T. Electrical conductivity and electromagnetic interference shielding efficiency of carbon nanotube/cellulose composite paper. Carbon 2008; 46:1253-69.

[12] Petrofesa NF, Gadallaa AM. Processing aspects of shaping advanced materials by electrical discharge machining. Advanced Materials and Manufacturing Processes 1998; 3(1):127-153.

[13] Efros AL, Shklovskii BI. Critical Behaviour of Conductivity and Dielectric Constant near the Metal-Non-Metal Transition Threshold. Phys Status Solidii B 1976; 76:475-85.

[14] Nan CW, Shen Y, Ma J. Physical Properties of Composites Near Percolation. Annu Rev Mater Res 2010; 40:131-51.

[15] Bauhofer W, Kovacs JZ. A review and analysis of electrical percolation in carbon nanotube polymer composites. Composites Science and Technology 2009; 69:1486–98.

[16] Stauffer D, Aharony A. Introduction to percolation theory. London: Taylor & Francis; 1992.

[17] Sahimi M. Applications of percolation theory. London: Taylor & Francis; 1994.

[18] Celzard A, McRae E, Deleuze C, Dufort M, Furdin G, Marẽché JF. Critical concentration in percolating systems containing a high-aspect-ratio filler. Phys Rev B 1996; 53(10):6209–14.

[19] Munson-McGee SH. Estimation of the critical concentration in an anisotropic percolation network. Phys Rev B 1991; 43:3331–6.

[20] Qin F, Brosseau C. A review and analysis of microwave absorption in polymer composites filled with carbonaceous particles. J. App. Phys. 2012 111 061301

[21] Sandler J, Shaffer MSP, Prasse T, Bauhofer W, Schulte K, Windle AH. Development of a dispersion process for carbon nanotubes in an epoxy matrix and the resulting electrical properties. Polymer 1999; 40:5967–71.

[22] Kilbride BE, Coleman JN, Fraysse J, Fournet P, Cadek M, Drury A, Hutzler S, Roth S, Blau WJ. Experimental observation of scaling laws for alternating current and direct current conductivity in polymer-carbon nanotube composite thin films. J Appl Phys 2002; 92(7):4024-30.

[23] Sandler JKW, Kirk JE, Kinloch IA, Shaffer MSP, Windle AH. Ultra-low electrical percolation threshold in carbon-nanotube-epoxy composites. Polymer 2003; 44(19):5893-99.

[24] Coleman JN, Curran S, Dalton AB, Davey AP, McCarthy B, Blau W, Barklie RC. Percolation-dominated conductivity in a conjugated-polymer-carbon-nanotube composite. Phys Rev B 1998; 58(12):7492–7495.

[25] Winey KI, Kasiwagi T, Mu M. Improving electrical conductivity and thermal properties of polymers by addition of carbon nanotubes as fillers. MRS Bull 2007; 32(4):348–53.

[26] Bryning MB, Islam MF, Kikkawa JM, YodhAG. Very low conductivity threshold in bulk isotropic single wall carbon nanotube epoxy composites. Adv Mater 2005; 17(9):1186–91.

[27] Yan MF, Cannon RW, Bowen HK "Grain boundary migration in ceramics" Ceramic Microstructures ´76" , Ed. R. M. Fulrath and J. A. Pask , Westview Press 1977, 276-307.

[28] Ezquerra TA, Connor MT, Roy S, Kulescza M, Fernandez-Nascimento J, Baltá-Calleja FJ, Alternating-current electrical properties of graphite, carbon-black and carbon-fiber polymeric composites. Comp. Sci. Techn. 2001 61 903-909

[29] Ostapchuk T, Petzelt J, Hlinka J, Bovtun V, Kuzel P, Ponomareva I, Lisenkov S, Bellaiche L, Tkach A, Vilarinho P. Broad-band dielectric spectroscopy and ferroelectric soft-mode response in the Ba0.6Sr0.4TiO3 solid solution. J Phys Cond Matter 2009; 21:474215/1-9.

[30] Gervais F, Pirou B. Anharmonicity in several-polar-mode crystals: adjusting phonon self-energy of LO and TO modes in Al2O3 and TiO2 to fit infrared reflectivity, J. Phys. C 1974, 7, 2374- 2386

[31] Pecharromán C, Iglesias JE. Effect of Particle Shape on the IR Reflectance Spectra of Pressed Powders of Anisotropic Materials. Appl Spectrosc 2000; 54(4):634-8.

[32] Pecharromán, C , Gracía, F, Holgado, J.P, Ocaña, M., González-Elipe, A.R., Bassas, J., Santiso, J., Figueras, A, Determination of texture by infrared spectroscopy in titanium oxide-anatase thin films, J.Appl. Phys., 2003, 93:4634-4645

[33] Schubert M, Tiwald TE, Herzinger CM. Infrared dielectric anisotropy and phonon modes of sapphire. Phys Rev B 2000; 61:8187-8201.

[34] Philipp HR, Infrared optical properties of graphite. Phys. Rev. B, 1977 16(6) 2896-2900.

[35] Draine BT, Lee HM, Optical-Properties Of Interstellar Graphite And Silicate Grains, Astrophys. J. 1984 285 89-108

[36] Swiatnicki, W., Lartigue-Korinek, S., Laval, J.Y., Grain boundary structure and intergranular segregation in Al2O3; Acta Metallurgica Et Materialia 199;5 43(2): 795-805

[37] Guilmeau, E., Chateigner, D., Suzuki, T.S., Sakka, Y., Henrist, C., Ouladdiaf, B. Rietveld texture analysis of alumina ceramics by neutron diffraction, Chemistry of Materials 2005; 17(1): 102-106.

[38] Pecharromán, C, Mata-Osoro, G, Díaz, L.A, Torrecillas, R, Moya, J.S, On the transparency of nanostructured alumina: Rayleigh-Gans model for anisotropic spheres, Optics Express 2009; 17(8): 6899-6912

[39] Kuzel P, Pashkin A, Kempa M, Kadlec F, Kamba S, Petzelt J. Time-Domain Terahertz Spectroscopy of SrBi2Ta2O9. Ferroelectrics 2004; 300:125–9.

[40] Petzelt J, Rychetsky I, Nuzhnyy D. Dynamic ferroelectric-like softening due to the conduction in disordered and inhomogeneous systems: Giant permittivity phenomena. Ferroelectrics 2012; 426:171-193.

[41] Dyre JC, Schroder TB. Universality of ac conduction in disordered solids. Rev. Mod. Phys. 2000; 72:873-892.

[42] Dutta AK. Electrical conductivity of single crystals of graphite. Phys. Rev. 1953; 90:187-192.

[43] Deprez N, Mc Lachlan DS. The analysis of the electrical conductivity of graphite powders during compaction. J. Phys. D: Appl. Phys. 1988; 21:101-107.

[44] Ewen PJS, Robertson JM. A percolation model of conduction in segregated systems of metallic and insulating materials: application to thick film resistors. J Phys D: Appl Phys 1981; 14(12):2253-68.

[45] Krivka I, Prokes J, Tobolkova E, Stejskal J. Application of percolation concepts to electrical conductivity of polyaniline–inorganic salt composites. J Mat Chem 1999; 9:2425-28.

[46] Pecharroman C, Iglesias JE. Modeling Particle Size and Clumping Effects in the IR Absorbance Spectra of Dilute Powders. Appl Spectrosc 1996; 50(12):1553-62

[47] Petzelt J, Rychetsky I, Nuzhnyy D. Dynamic Ferroelectric–Like Softening Due to the Conduction in Disordered and Inhomogeneous Systems: Giant Permittivity Phenomena. Ferroelectrics 2012; 426:171-193.

[48] Maxwell-Garnett JC. Colours in Metal Glasses and in Metallic Films. Philos. Trans. R. Soc. Ser. A 1904; 203:385-420.

[49] Maxwell-Garnett JC. Colours in Metal Glasses, in Metallic Films, and in Metallic Solutions. II. Philos. Trans. R. Soc. Ser. A 1906; 205:237-288.

[50] Pecharroman C, Gonzalez Carreño T, Iglesias JE. Average Dielectric Constant of Coated Spheres: Application to the IR Absorption Spectra of NiO and MgO. Appl Spectros 1993; 47(8):1203-8.

[51] Jiang MJ, Dang ZM, Bozlar M, Miomandre F, Bai J. Broad-frequency dielectric behaviors in multiwalled carbon nanotube/rubber nanocomposites. J App Phys 2009 106, 084902-1-6

[52] Li YC, Li RKY, and Tjong S. Electrical transport properties of graphite sheets doped polyvinylidene fluoride nanocomposites. J. Mater. Res., 2010 25(8) 1645-8

[53] Panwar V, Kang B, Park JO, Park S, Mehra R.M, Study of dielectric properties of styrene-acrylonitrile graphite sheets composites in low and high frequency region. Euro. Pol. J. 2009 45 1777–1784

[54] Hotta M, Hayashi M, Lanagan MT, Agrawal DK and Nagata K, Complex Permittivity of Graphite, Carbon Black and Coal Powders in the Ranges of X-band Frequencies (8.2 to 12.4 GHz) and between 1 and 10 GHz. ISIJ Intern. 2011 51(11) 1766–1772

[55] Williams G and Watt DC. Non symmetrical dielectric relaxation behavior arising from a simple empirical decay function. Trans Faraday Soc 1970 66 80-85